

II.B.2 Solar High-Temperature Water-Splitting Cycle with Quantum Boost

Robin Taylor (Primary Contact), Roger Davenport, David Genders¹, Peter Symons¹, Lloyd Brown², Jan Talbot³, Richard Herz³

Science Applications International, Corp. (SAIC)
10260 Campus Point Drive
San Diego, CA 92121
Phone: (858) 826-9124
Email: taylorro@saic.com

DOE Managers

Sara Dillich
Phone: (202) 586-7925
Email: Sara.Dillich@ee.doe.gov

Katie Randolph
Phone: (720) 356-1759
Email: Katie.Randolph@go.doe.gov

Contract Number: DE-FG36-07GO17002

Subcontractors:

¹ Electrosynthesis Co., Inc. (ESC), Lancaster, NY

² Thermochemical Engineering Solutions (TCHEME), San Diego, CA

³ University of California, San Diego (UCSD), San Diego, CA

Project Start Date: September 1, 2007

Project End Date: January 31, 2014

- (<0.8 V) and/or identifying alternate membranes that can operate at higher temperature (up to 130°C) to take advantage of the lower thermochemical potential at higher temperature, but without an unacceptably high flux of sulfite across the membrane (<0.1 mmole/m²/s).
- Use the Aspen Plus[®] modeling tool to optimize systems for input to the H2A economic model. Evaluate using heat from excess electricity production for SO₃ decomposition. Evaluate power recovery and electrical power generation alternatives.
- Perform technical and economic analyses of the SA cycle systems with and without a high-temperature storage system that would allow for 24/7 operation.

Technical Barriers

This project addresses the following technical barriers from the Hydrogen Production section (3.1.5) of the Fuel Cell Technologies Office Multi-Year Research, Development, and Demonstration Plan:

- (S) High-Temperature Robust Materials
- (T) Coupling Concentrated Solar Energy and Thermochemical Cycles
- (U) Concentrated Solar Energy Capital Cost
- (V) Heliostat Development and Cost
- (Y) Diurnal Operation
- (Z) Control and Safety
- (AB) Chemical and Thermal Storage
- (AC) Solar Receiver and Reactor Interface Development

Technical Targets

Table 1 presents the progress made, to date, in achieving the DOE technical targets as outlined in the Multi-Year Research, Development, and Demonstration Plan – Planned Program Activities for 2005-2015 (updated July 2013), Table 3.1.7/7.A: Solar-Driven High-Temperature Thermochemical Hydrogen Production.

FY 2013 Accomplishments

- Long-term stability of the complete electrochemical system was demonstrated, including a >500 hour durability run.
- New membranes for the electrolytic cell have been identified with up to 2 orders of magnitude lower sulfite fluxes.

Overall Objectives

- Prove the viability of a sulfur family thermochemical water-splitting cycle for large-scale hydrogen production using solar energy.
- Evaluate sulfur ammonia (SA) water-splitting cycles that employ photocatalytic (quantum boost) or electrolytic hydrogen evolution steps and perform lab testing to demonstrate feasibility of the chemistry.
- Perform economic analyses of SA cycles as they evolve.
- Develop a cycle that has high potential for meeting the DOE threshold cost goal of \$2-4/kg H₂ and solar-to-hydrogen (STH) energy conversion ultimate target of 26%.

Fiscal Year (FY) 2013 Objectives

- Improve electrolytic H₂ production by developing better anode electrocatalysts to facilitate operation at lower temperatures (80°C) while maintaining low voltage

TABLE 1. Progress towards Meeting Technical Targets for Solar-Driven High-Temperature Thermochemical Hydrogen Production

Characteristics	Units	U.S. DOE Targets ^a			Project Status
		2015	2020	Ultimate	
Solar-Driven High-Temperature Thermochemical Cycle Hydrogen Cost	\$/kg H ₂	14.80	3.70	2.00	10.91 ^b (2015) 7.04 ^b (2025)
Heliostat Capital Cost (installed cost)	\$/m ²	140	75	75	97 ^c
Chemical Process Energy Efficiency ^d	%	25	30	>35	20
STH Energy Conversion Ratio ^e	%	10	20	26	9.6

^a Source: Multi-Year Research, Development, and Demonstration Plan (Updated July 2013) <http://www1.eere.energy.gov/hydrogenandfuelcells/mypp/pdfs/production.pdf>

^b Electrolytic system projected costs based on latest H2A analysis.

^c Based on SAIC glass-reinforced concrete structure with 10 sq.m. area and low production quantity.

^d Chemical process efficiency is defined as the energy of the hydrogen produced (lower heating value, LHV) divided by the sum of the energy delivered by the solar concentrator system plus any other net energy imports (electricity or heat) required for the process.

^e STH energy conversion ratio is the overall system efficiency defined as the LHV of the hydrogen produced divided by the sum of the solar energy incident on the solar collector field and any other net energy imports. The estimated solar field efficiency to provide 800°C energy to the storage system is 48% based on the National Renewable Energy Laboratory Solar Advisor Model calculations.

- Separation of NH₃ and SO₃ in the oxygen generation step was demonstrated using a sulfate/pyrosulfate molten salt system.
- Lower melting temperatures were achieved with a combination of sodium salts and potassium salts.
- The molten salt viscosity was measured to be low (<5.5 cP at 450°C), proving that it can be easily pumped.
- Aspen Plus[®] was used to model significant process improvements, including:
 - A phase-change thermal-storage system with NaCl incorporated, allowing 24/7 continuous plant operation.
 - Rankine power cycles were designed to recover excess heat and efficiently generate electricity.
 - Overall plant pressure and SO₃ decomposer temperature were varied to optimize plant efficiency and power recovery.
- The focus of the solar configuration was determined to be a 50 MW_{th} central receiver system with NaCl molten salt storage to allow 24/7 operation and produce 5,400 kg/day of H₂ per module.
- The H2A version 3 economic model was used to optimize and trade off SA cycle configurations.



INTRODUCTION

Thermochemical production of hydrogen by splitting water with solar energy is a sustainable and renewable method of producing hydrogen. However, the process must be proven to be efficient and cost-effective if it is to compete with conventional energy sources.

APPROACH

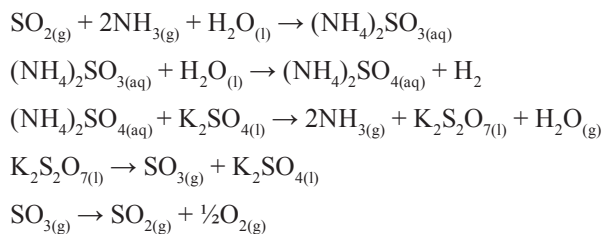
To achieve the project objectives, a variation of the hybrid sulfur thermochemical water splitting cycle (*aka* the “Hybrid Sulfur,” or “HyS” cycle) was developed by introducing ammonia as a working reagent (thus “sulfur-ammonia,” or “SA,” cycle) to allow more efficient solar interface and facile product separation steps. The thermochemical cycle SA process was originally developed by the Florida Solar Energy Center. Several versions of the SA cycle have been evaluated, both experimentally and analytically.

Two approaches were considered for the hydrogen production step of the SA cycle: photocatalytic and electrolytic oxidation of ammonium sulfite to ammonium sulfate in an aqueous solution. Also, two sub-cycles have been considered for the oxygen evolution side of the SA cycle: zinc sulfate/zinc oxide and potassium sulfate/potassium pyrosulfate sub-cycles. The laboratory testing and optimization of all the process steps for each version of the SA cycle were then carried out. Once the optimum configuration of the SA cycle has been identified and the cycle has been validated in closed loop operation in the lab, it will be ready to be scaled up and tested on-sun.

RESULTS

Cycle Evaluation and Analysis

During the past year, work focused on the electrolytic SA cycle, which is summarized in the following equations:



- 1 - chemical absorption 110-160°C
- 2 - electrolytic 80-150°C
- 3 – adiabatic mixing 400-450°C
- 4 – stored thermal 790°C
- 5 – electric heat 850-1200°C

The electrolytic oxidation of the ammonium sulfite solution occurs more efficiently at higher temperatures, requiring the development of a system capable of running at higher pressures. Reactions (3) and (4) form a sub-cycle by which potassium sulfate is reacted with ammonium sulfate in the low-temperature reactor, to form potassium pyrosulfate. That substance is then fed to the medium-temperature reactor, where it is decomposed to SO₃ and K₂SO₄ again, closing the sub-cycle. The potassium sulfate and pyrosulfate form a miscible liquid melt that facilitates the separations and the movement of the chemicals in reactions (3) and (4). The oxygen production step (5) occurs at high temperature over a catalyst. Separation of the oxygen from SO₂ occurs when they are mixed with water in reaction (1). The net cycle reaction represented by reactions 1-5 is the decomposition of water to form hydrogen and oxygen. All of the reaction steps described above have been demonstrated in the laboratory and shown to occur without undesirable side reactions. However, we are working to ensure that there are none in the electrolytic step and the SO₃ decomposition. Figure 1 shows a schematic of the electrolytic SA cycle.

Electro-Oxidation of Aqueous Ammonium Sulfite Solutions

A 500-hour durability test was successfully completed using an electrochemical cell comprising a Pt/Co catalyzed anode on a carbon felt substrate and a Pt/C membrane electrode assembly cathode on a FuMaTech FX-7050 cation exchange membrane. The test was run at 100 mA/cm² for a total of 550 hours electrolysis time at a temperature of 100°C, which required the use of a pressurized cell reactor. The durability testing was done as four consecutive batch electrolyses, with each experiment being run to approximately 90% conversion of sulfite to sulfate. The coulombic efficiency for hydrogen production was 94%, and the cell voltage increased reproducibly and consistently over each batch by an amount predicted from thermodynamic calculations based on the conversion (1.09–1.17 V). Figure 2 shows excellent reproducibility for the change in concentration of sulfite for the four consecutive batches as a function of charge passed. Note that as the electrolysis proceeds, there is also a concentrating effect in the anolyte as water transfer accompanies the transport of cations across the cation exchange membrane. We measured the water transfer rate to

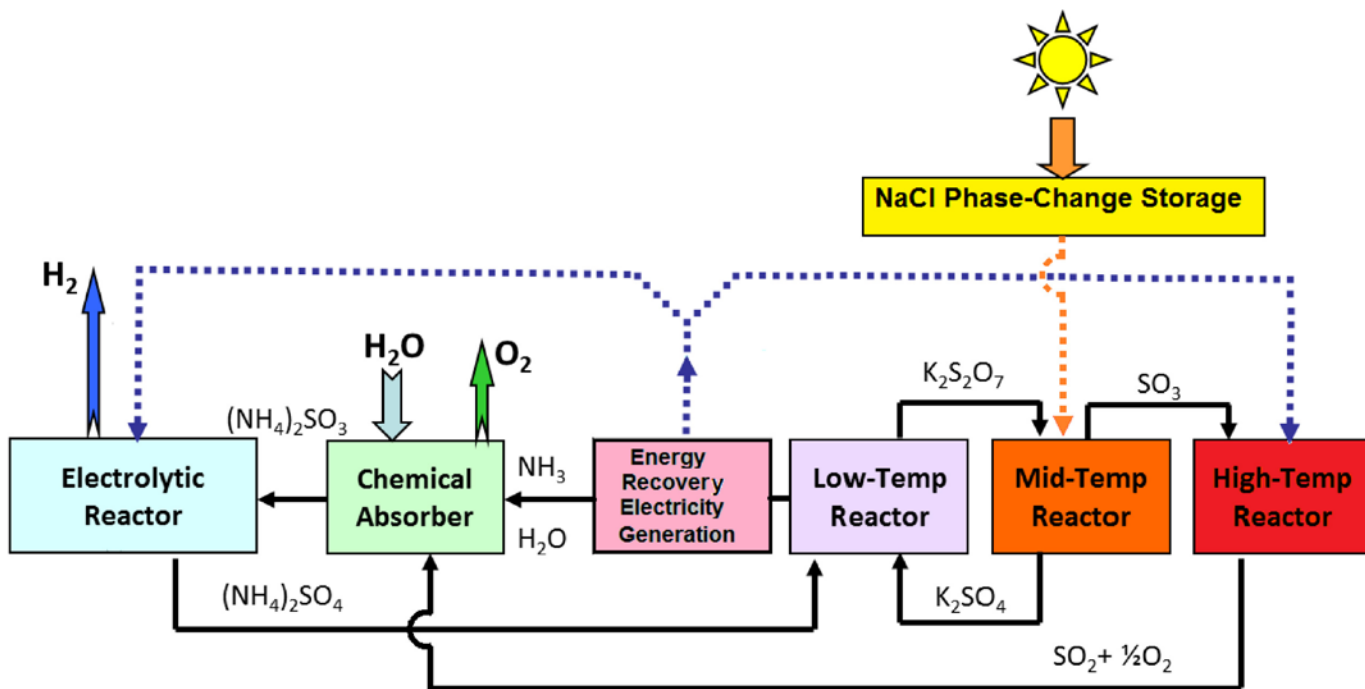


FIGURE 1. Schematic of the Electrolytic SA Cycle

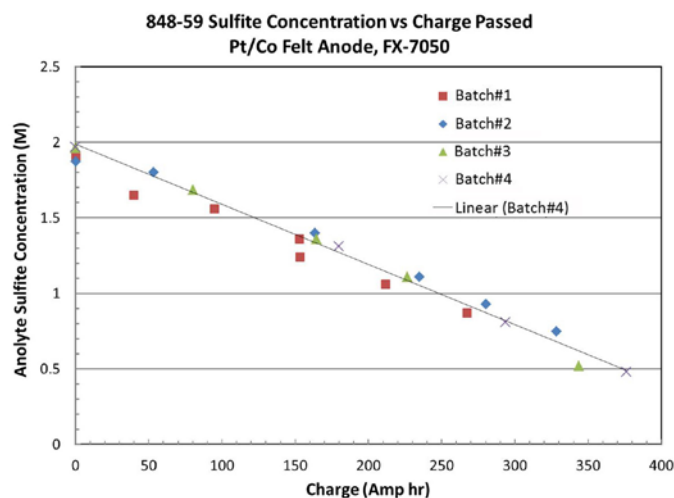


FIGURE 2. Electrochemical Oxidation of Sulfite—Plot of Sulfite Concentration vs. Charge for Four Separate Batches Totalling 550 Hours

be 3.1 moles/mole of charge passed, which is consistent with observations in other electrochemical systems.

The purpose of the durability test was to demonstrate the stability of the electrocatalysts and the membrane. This can be assessed by looking for changes in coulombic efficiency and cell voltage as a function of electrolysis time. The coulombic efficiencies were consistent over the entire run. Given the small changes in cell voltage as a function of conversion, the cell voltage needs to be compared for the same anolyte conversion for each batch. This was done towards the end of each batch and showed that the cell voltage was 1.139 V \pm 6 mV, or 0.5% variation between batches, again showing excellent stability over the 550-hour test.

Previous attempts to run durability tests at elevated temperature (100-130°C) were abandoned due to high sulfite transfer and subsequent reaction at the cathode. Using the FX-7050 membrane, the sulfite flux averaged 1.7×10^{-4} mole/m²-s over the entire test. Since running the long-term test, we have evaluated a developmental membrane from DuPont that, in short-term testing, has shown up to two orders of magnitude reduction in sulfite flux. Initial testing in the electrolysis rig at 85°C showed this membrane gave up to 25% lower cell voltage than the cell with the FX-7050 membrane used in the long-term testing. However, attempts to use the membrane at 130°C showed a slow increase in the cell voltage, possibly due to dehydration of the membrane. Further work is required to characterize this phenomenon and understand the reasons for the apparent increase in resistance. Despite the increase in cell voltage, the coulombic efficiency for hydrogen production was very good (>95%), and the measured total flux of sulfur species was 8×10^{-5} mol/m²-s.

UCSD synthesized cobalt ferrite and platinum cobalt nanoparticles and then used electrophoretic deposition (EPD)

with two new suspension chemistries that produced thinner and more distributed layers of the catalysts. Cobalt ferrite nanoparticles were synthesized using a co-precipitation method [1]. The samples were analyzed using a scanning electron microscope (SEM), which showed particles from 4-20 nm, and an energy-dispersive X-ray spectroscopy to verify composition. Pt₃Co was synthesized using a solvothermal process [2] in which nanoparticles formed in a sealed autoclave; the particle size of 20 ± 5 nm was measured using an SEM image. Nanoparticles of 30 wt% platinum cobalt on carbon were also purchased from Sigma Aldrich. SEM images showed that the Pt₃Co-loaded carbon particle size was 50 ± 15 nm.

The first EPD bath contained 2 g/L particles suspended in 90 vol% water and 10 vol% isopropanol with 0.4 g/L hexadecyltrimethylammonium bromide (CTAB). Figure 3 compares the zeta potential of cobalt ferrite in 90 vol% water and 10 vol% isopropanol solution with and without CTAB as a function of pH as changed with the addition of nitric acid and sodium hydroxide. The zeta potential was only positive at low pH without CTAB, but remained positive with addition of CTAB over a wide range of pH values. The second bath contained 2 g/L particles suspended in 100% ethanol. The zeta potential of the cobalt ferrite nanoparticles in the CTAB bath chemistry at a pH of 6.2 was 20 ± 2 mV.

EPD of both cobalt ferrite and platinum cobalt nanoparticles was achieved from two different bath chemistries. Cobalt ferrite deposits from a 100% ethanol bath at a pH of 5 gave a 3-5 layer deposit that was evenly distributed across the substrate. This EPD method will be used to deposit particles on graphite paper to further test the electrocatalytic properties of the particles themselves. The platinum cobalt particles on carbon were large and deposited in small agglomerates from both tested baths. Sonication of the bath during EPD resulted in smaller agglomerates that were more evenly distributed in comparison with deposits conducted without sonication.

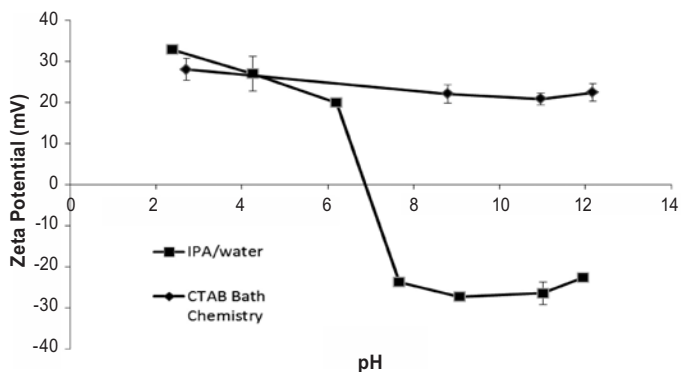


FIGURE 3. Zeta Potential vs. pH for Cobalt Ferrite Particles in a 90 vol% Water, 10 vol% Isopropanol Alcohol Solution and in a CTAB Solution

The deposits were tested for electrocatalytic properties for the oxidation of ammonium sulfite to ammonium sulfate. Linear sweep voltammetry was used to compare the electrocatalytic activity of cobalt ferrite and platinum cobalt nanoparticles deposited on graphite paper using EPD. Cobalt ferrite was deposited at 35 V for 60 s from a 100% ethanol bath. Platinum cobalt was deposited with an applied voltage of 13 V for 15 s from a CTAB bath. The deposit densities varied from 0.3 mg/cm² to 0.8 mg/cm² depending upon the EPD bath chemistry and material deposited. As shown in Figure 4, both cobalt ferrite and platinum cobalt nanoparticle deposits show enhanced electrochemical activity compared to graphite paper, that is, a higher current density for all voltages scanned. As the particle size and loading of the cobalt ferrite and platinum cobalt nanoparticles are different, it is difficult to directly compare their electrocatalytic activity, which will be done in future work. Electrosynthesis has been conducted using our electrophoretic deposition procedure to test other possible catalysts.

High-Temperature Cycle Step Evaluation

Experimental work was completed demonstrating that the all-liquid/gas high-temperature cycle steps are feasible. Specifically, the decomposition steps to evolve NH₃ and SO₃ occur at sufficiently different temperatures, the molten salts are liquid and are pumpable at the conditions required, and the melting point of the molten salts can be adjusted by addition of sodium salts to the potassium salt mixture. Specifically, experiments were conducted to show the evolution of ammonia and water vapor at ~465°C, followed by evolution of sulfur trioxide at 500°C. It was determined that it should be easy to pump these molten salts with viscosities below 5.5 cP at 450°C.

Aspen Plus® Process Analysis

The chemical process remains basically unchanged but with significant improvement in the thermal integration of the process. The major source of electrical energy used for

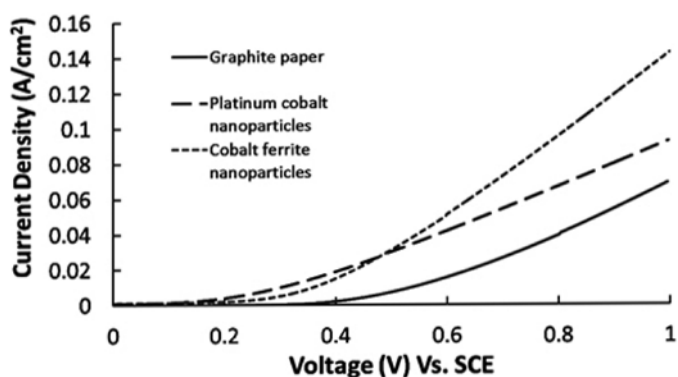


FIGURE 4. Electrocatalytic Activity of EPD Deposits Showing Current Density vs. Voltage

electrolysis and electrically heated SO₃ decomposition is energy recovered from the ammonia-steam product of the low-temperature reactor. Previously, we had employed a turbine to recover this energy, but the small amount of SO₂ in the stream will result in the formation of solids in the turbine, which is unacceptable. We now use heat exchange to a separate waste heat recovery system. A trade-off analysis was undertaken to determine which working fluid would provide the highest efficiency for this system. Although water could be used, a lower boiling working fluid would give higher efficiency. Ammonia and sulfur dioxide are obvious alternatives since they are already in use in the plant and cross-contamination from heat exchanger leakage would not result in undesirable or reactive byproducts. An ammonia water mixture was also considered. Ultimately, ammonia was chosen as the working fluid as it gave a good thermal match to the source stream with minimal process complications.

UCSD improved the Aspen Plus® model of the plant. A process heat integration analysis, or pinch analysis, of the plant was performed in order to place heat exchangers at optimal positions. Thermodynamic data from the literature were incorporated into the mid-temperature reactor, which decomposes molten pyrosulfates to sulfates and releases gaseous SO₃. Calculator blocks were utilized to obtain power requirements for the electrolyzer and the overall efficiency of the plant. Design specifications were placed in strategic areas of the model to aid convergence.

Figure 5 shows an overview of the latest Aspen Plus® model of the plant. Not shown is a thermal storage system that allows 24/7 operation of the plant. In the thermal storage system, the latent heat of NaCl melting and solidifying stores and releases solar thermal energy for use by the plant at night. NaCl melts at 801°C; thus, the endothermic mid-temperature reactor is operated at 790°C in order to provide heat transfer from the thermal storage system to the plant. The low-temperature reactor operates adiabatically at 400°C. The endothermic high-temperature reactor is heated electrically to 950°C by resistive heaters powered by power plants that recover heat within the main process plant and generate electricity. Two Rankine-cycle electrical power plants are coupled to the main process plant through heat exchangers. The working fluid in the Rankine-cycle power plants was selected to be ammonia in order to match the temperatures and phase changes in the process streams of the main plant. The power plant at the top of the figure recovers energy from cooling and condensation of the ammonia/water product of the low-temperature reactor. The power plant in the bottom-right of the figure recovers energy from resistive heating in the electrolyzer.

The total heat requirements of the solar reactors along with the total hydrogen product were exported to a calculator block that computes the overall efficiency of the plant. Currently, the overall process efficiency is 20%. It is anticipated that the efficiency can be increased to 28–30%

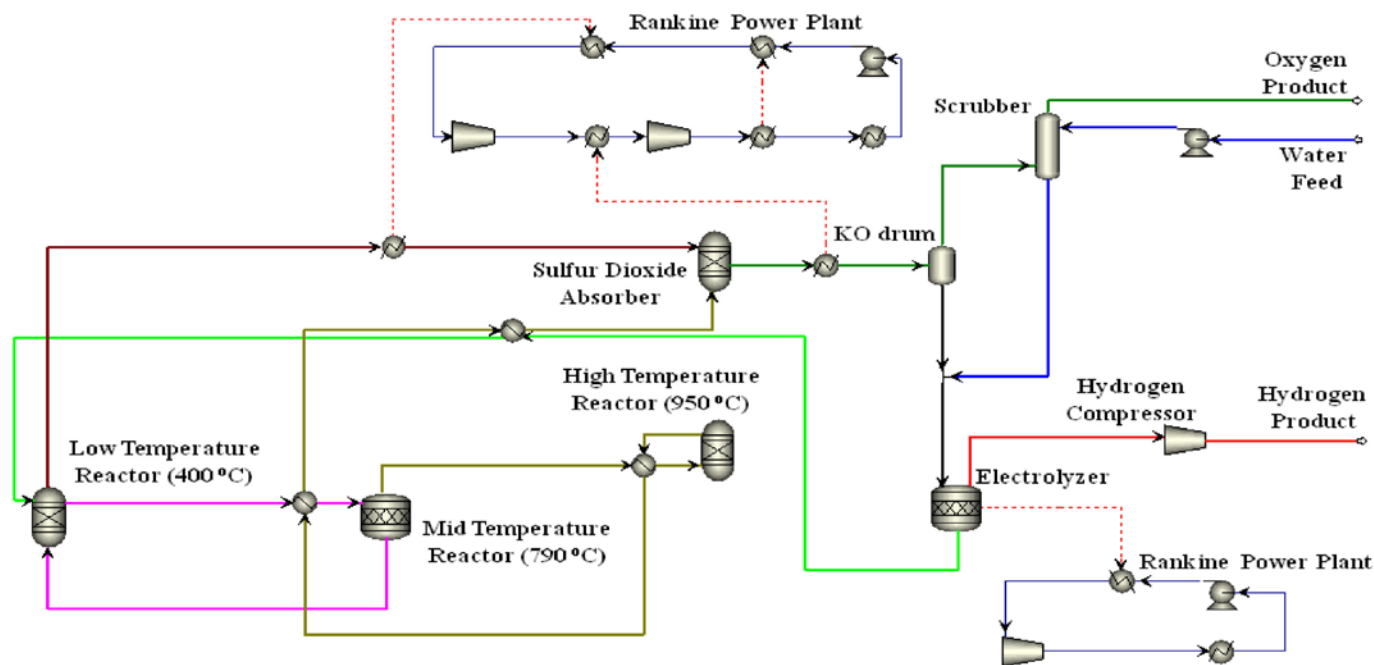


FIGURE 5. Overview of the Aspen Plus® Model

with further refinement of the heat integration and power generation portions of the system and improvement in the electrolytic process performance.

Heat Storage

To allow the chemical plant to operate 24/7, storage of solar energy is needed, and the most efficient type of storage is direct thermal storage. To provide the needs of the medium-temperature reactor, a maximum temperature of about 800°C is needed. SAIC identified a unique phase-change storage approach using molten NaCl that provides large amounts of thermal capacity (481 kJ/kg) at this temperature, as well as providing an efficient means of extracting the heat from the storage to the molten salts [3,4]. The storage consists of a tank holding a volume of NaCl, with headspace above to accommodate the expansion/contraction of the salt as it changes phase. A schematic of the conceptual system is shown in Figure 6. A thin layer of liquid sodium metal (Na) floats on top of the molten NaCl, and the headspace is filled with Na vapor at its vapor pressure, which runs from about 0.5 to 1.5 bar over the temperature range expected. Pipes carrying the molten salt materials to be heated pass through the headspace in contact with the Na vapor, and the sodium acts as a heat pipe to transfer heat from the NaCl to the pipes. Solid NaCl that forms in the Na pool sinks to the bottom (there is about a 30% reduction in volume upon solidification), so the Na remains in contact with liquid NaCl as the entire heat capacity of the storage is used. To re-melt the NaCl, pipes containing liquid sodium are placed at the bottom of the tank, and circulation from the solar receiver heats and re-melts the NaCl.

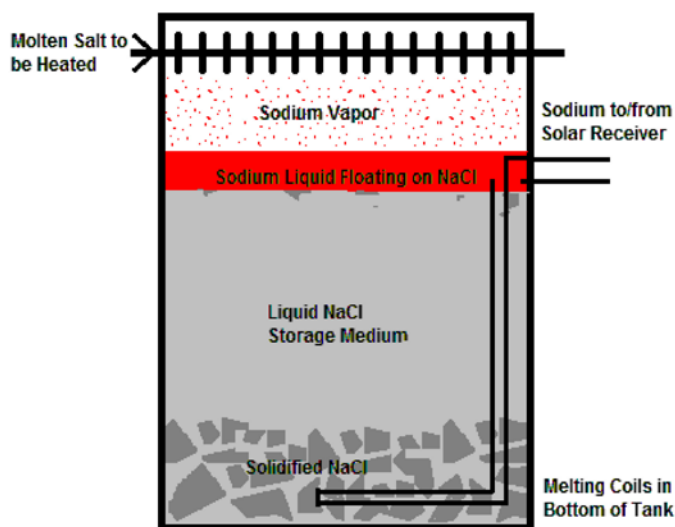


FIGURE 6. Schematic of a Conceptual NaCl Heat Storage System

SAIC summer interns from UCSD have continued to investigate the thermal storage system. Interaction with other researchers has indicated there can be problems of crust formation in the NaCl upon freezing, and ideas to mitigate this have been developed. The students are designing a demonstration testing approach that could be performed on the SAIC solar dish. Configurations with a sodium heat pipe receiver and with a sodium pumped loop have been studied (see Figure 7). Also, analogue testing with low-temperature phase-change materials is being developed to study freeze/thaw behavior and other features of the system at a bench scale.

Solar Field Optimization

A modular solar plant configured to deliver thermal power to the modular 50-MW_{th} chemical plant has been designed (see Figure 8). The central receiver solar plant includes a north-side heliostat field with 227,600 square meters of heliostats. The heliostats focus onto a 150-meter-tall tower with a cavity receiver about 12 m x 14 m in size. Energy absorbed at the receiver is delivered to the NaCl phase-change storage system at about 800°C. Performance estimates indicate a 150-MW_{th} peak absorbed power for the system, 1,196 MWh peak daily energy collection (equivalent to 50 MW_{th} continuously over 24 hours), and 32.3 MW_{th} average power over the year (65% overall capacity factor). The overall average efficiency of the solar plant, from incident solar energy to delivered thermal energy, was estimated at 48% using the National Renewable Energy Laboratory Solar Advisor Model.

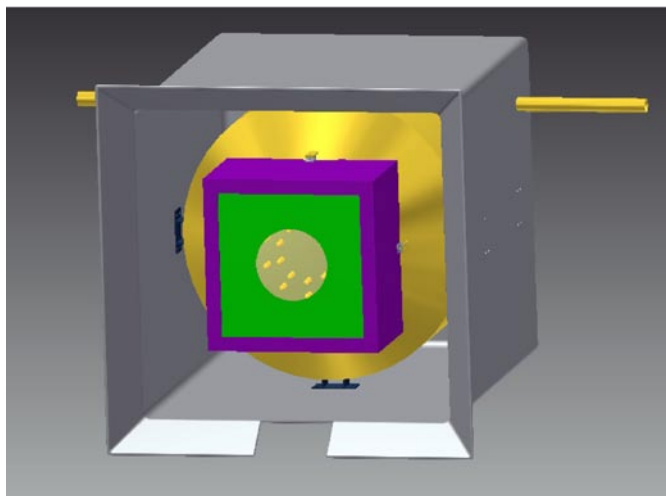


FIGURE 7. Schematic of a Heat Pipe Receiver with On-Dish NaCl Storage for Dish Demonstration

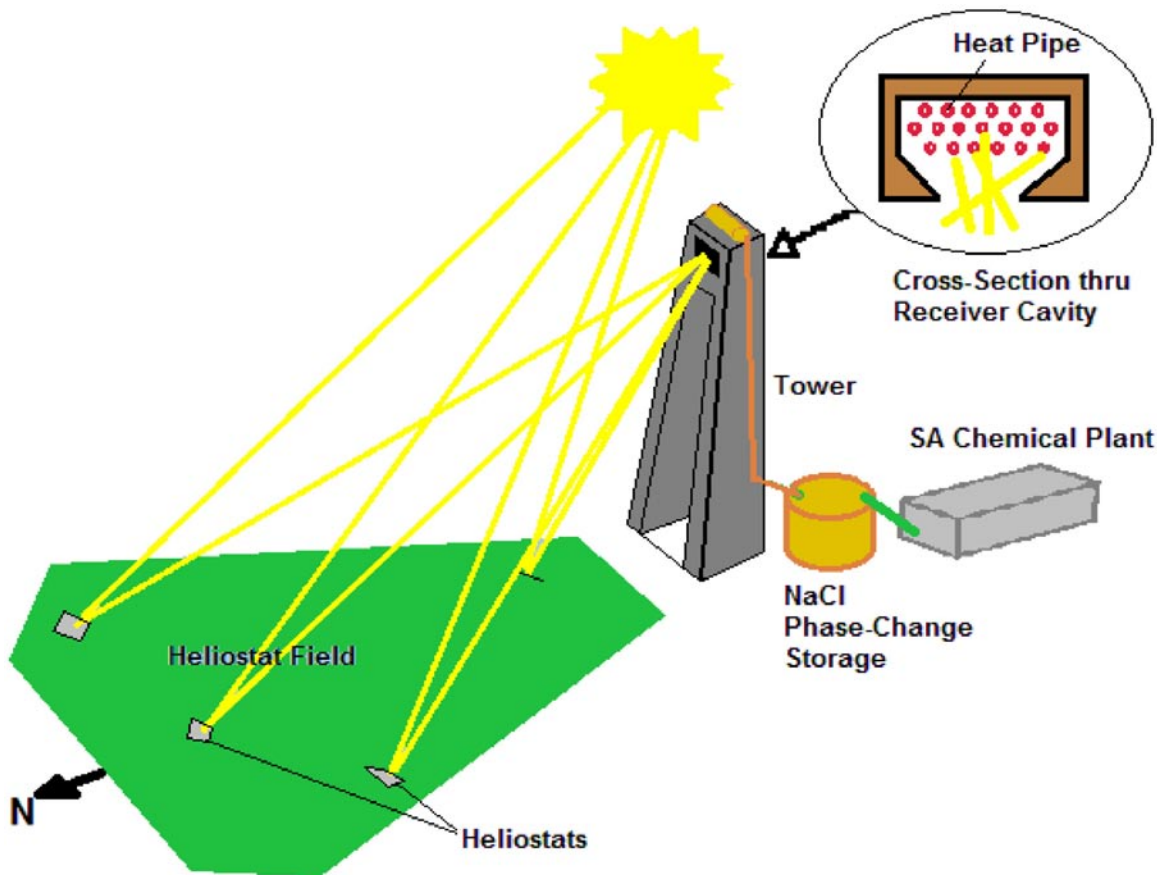


FIGURE 8. Schematic of 50-MW_{th} SA Hydrogen Production System Configuration

Economic Analysis

The H2A economic analysis was converted to version 3 of H2A, and the plant costs were updated with the most up-to-date estimates of plant and solar equipment costs, based on the 50-MW_{th} unit size. The results were a \$53 million solar module cost (including NaCl storage) and a \$17 million process plant cost. The 50-MW_{th} plant produces about 5,400 kg of hydrogen per day; thus, 19 plants would be needed to meet the DOE production level of 100,000 kg/day. The itemized 2015 and total 2025 production cost of hydrogen from this plant is shown in the following table:

Cost Component	Hydrogen Cost (\$/kg)	Fraction of Total Cost
Capital Cost	8.96	82%
Fixed O&M	1.90	17%
Other	0.05	1%
Total 2015	10.91	
Total 2025	7.04	

O&M – operations and maintenance

The estimated hydrogen production cost for 2025 decreases to \$7.04/kg based on reductions in heliostat costs and improvements in the efficiency of the chemical and electrochemical portions of the system.

CONCLUSIONS AND FUTURE DIRECTIONS

In summary:

- The SA cycle is unique in that it is an all-fluid cycle with no high-temperature solids handling. It is a relatively low-temperature plant. The solar receiver operates at 800°C when the SO₃ decomposition is achieved through electrical heating with excess electricity production of the system. All the electricity needed for the process is generated internally, and the cycle can operate 24/7 with low-cost storage.
- The long-term stability of the electrochemical system was demonstrated with a 500+ hour extended run; however, not at the optimum operating conditions. A lower temperature was used since sulfite fluxes were found to be too high at 130°C. Recently, alternate membranes were identified with up to 2 orders of magnitude lower sulfite fluxes even at higher temperatures. Durability of these membranes still needs to be evaluated.
- Experiments for the oxygen evolution sub-cycle using potassium sulfate confirmed that ammonia and sulfur trioxide can be evolved separately with a 25–50°C temperature difference, thus avoiding difficult gas separation processes. The melting points, densities, and viscosities of the K₂SO₄/K₂S₂O₇ molten salts

were measured to prove that they have low viscosities and can be easily pumped. It was confirmed that the decomposition of SO₃ is proven technology, thus laboratory demonstration was not necessary. The entire process consists of elementary chemical engineering unit operations, all in widespread industrial use for over 100 years.

- The Aspen Plus® SA process modeling showed that a phase-change thermal-storage system with NaCl incorporated would allow 24/7 continuous plant operation. Rankine power cycles were modeled to recover excess heat and efficiently generate electricity. Overall plant pressure and SO₃ decomposer temperature were varied to optimize plant efficiency and power recovery.
- The solar configuration was focused on a 50-MW_{th} central receiver system with NaCl molten salt storage to allow 24/7 operation and produce 5,400 kg/day H₂ per module, thus requiring 19 modules to produce 100,000 kg/day H₂.
- The H2A economic analysis was converted to version 3 of H2A, and the plant costs were updated with the most up-to-date estimates of plant and solar equipment costs, based on the 50-MW_{th} module size.

Activities planned for the upcoming year include:

- Continue optimization of the electrolytic process through catalyst development and alternate membrane screening. With catalyst development, the objectives are to lower the anode over-potential at high current densities, increase effective catalyst surface area using nanoparticles, and increase the cathode hydrogen selectivity in the presence of sulfite. Achieve high-temperature operation with low sulfite flux through alternate membrane screening.
- Continue refinement of the Aspen Plus® model to maximize hydrogen production efficiency, perform trade-off studies of power recovery options, and provide input to the H2A economic model.
- Continue to evaluate NaCl phase-change storage system configuration, materials, and components to achieve 24/7 operation.
- Continue to update the H2A analysis to improve the quality of cost estimates through initial design of key process equipment.

FY 2013 PUBLICATIONS/PRESENTATIONS

- Taylor, R., Genders, D., Brown, L., Talbot, J., Herz, R., Davenport, R., Presentation at the STCH Hydrogen Production Technology Team Review Meeting, La Jolla, California, July 10, 2012. (PowerPoint presentation).

2. Taylor, R., Genders, D., Brown, L., Talbot, J., Herz, R., Davenport, R., Presentation at the DOE Sulfur Ammonia Cycle Phase 1 Go/No-Go Meeting Teleconference, August 27, 2012. (PowerPoint presentation).
3. Tanakit, R., Luc, W., Solar Hydrogen Project, Presentation at the SAIC/UCSD Jacobs School of Engineering Intern Summit, San Diego, California, September 14, 2012. (PowerPoint presentation).
4. Tanakit, R., Luc, W., Solar Hydrogen Project, Poster presentation at the UCSD Jacobs School of Engineering Corporate Affiliates Program, La Jolla, California, September 27, 2012.
5. J. Littlefield, "Solar Thermochemical Hydrogen Production Plant Design," M.S. thesis, (2012). Thesis defense on Nov. 19, 2012.
6. Jesse Littlefield, Mimi Wang, Lloyd C. Brown, Richard K. Herz, and Jan B. Talbot, "Process Modeling and Thermochemical Experimental Analysis of a Solar Sulfur Ammonia Hydrogen Production Cycle," World Hydrogen Energy Conference 2012, *Energy Procedia* 29 (2012) 616 – 623.
7. Wesley W. Luc, Richard K. Herz, and Jan B. Talbot, "Design of a Solar Thermochemical Hydrogen Production Plant," Poster presented at the UCSD Jacobs School of Engineering Research Expo, April 18, 2013.
8. Brown, L., Symons, P., Taylor, R., Presentation at the 2013 U.S. DOE Hydrogen and Fuel Cell Program and Vehicle Technologies Program Annual Merit Review and Peer Evaluation Meeting, Washington, D.C., May 16, 2013. (PowerPoint presentation).
9. Luc, W., "A Continuous Solar Thermochemical Hydrogen Production Plant Design," M.S. thesis, University of California, San Diego, 2013.

10. Taylor, R., Davenport, R., Genders, D., Symons, P., Herz, R., Talbot, J., Brown, L., Luc, W., "Status of the Solar Sulfur Ammonia Thermochemical Hydrogen Production System for Splitting Water," Technical Paper to be presented at the SolarPACES 2013 Conference, Las Vegas, Nevada, September 17–20, 2013.
11. Ryan Tanakit, Wesley Luc, J. Talbot, "Electrophoretic Deposition of Cobalt Ferrite and Platinum Cobalt Nanoparticles as Electrocatalysts," Abstract 2306, for presentation at the 224th ECS Meeting in San Francisco, California (October 27 – November 1, 2013).

REFERENCES

1. Z. Zi, Y. Sun, X. Zhu, Z. Yang, J. Dai, and W. Song, *Journal of Magnetism and Magnetic Materials*, **321**, 1251-1255 (2009).
2. Wang, W.; Wang, G.; van der Vliet, D.; Chang, K.; Markovic, N.; Stamenkovic, V., Monodisperse Pt₃Co nanoparticles as electrocatalyst: the effects of particle size and pretreatment on electrocatalytic reduction of oxygen. *Physical Chemistry Chemical Physics*. **2010**, *12*, 6877-7296.
3. Adinberg, R.; Yogeve, A.; Kaftori, D., High Temperature Thermal Energy Storage an Experimental Study, *J. Phys. IV France* 9, 1999.
4. White, M.; Qiu, S.; Galbraith, R., Phase Change Salt Thermal Energy Storage for Dish Stirling Solar Power Systems. ASME 2013 7th International Conference on Energy Sustainability. 2013, Paper No. 18292.